

IRRADIATION EFFECTS IN PICOSECOND LASER MATERIALS PROCESSING

DANA MIU, C. GRIGORIU, I. NICOLAE

National Institute for Laser, Plasma and Radiation Physics, 409 Atomistilor St., Bucharest-Magurele,
Romania, E-mail: miu@ifin.nipne.ro, grigoriu@ifin.nipne.ro, ionut@ifin.nipne.ro

(Received June 7, 2010)

Abstract. Effects of the irradiation of stainless steel and silicon using picosecond laser pulses are presented. Characteristic ripples are obtained for both materials. Results for various target scanning conditions are explained by polarization and incubation. The dissimilarities in morphology are due to the different ablation regimes. The implications of the observed phenomena for applications are discussed.

Key words: laser irradiation, picosecond pulses, materials processing, ablation, ripples, polarization, incubation.

1. INTRODUCTION

Research on the effects of laser irradiation of various materials has been undertaken since the discovery of the laser [1 – 3]. Interest has been spurred by the numerous applications of the laser in materials processing (cutting, drilling, welding, etc.). The advent of short pulse lasers in the fs (10^{-15} s) and ps (10^{-12} s) domain has opened up new areas of research, related both to the physical phenomena involved and to applications. Much of the research has been related to femtosecond lasers [4, 5]. However, picosecond lasers have many advantages for materials processing applications, making them more attractive than fs lasers in many applications [6, 7]: they are cheaper, more sturdy and better suited for industrial conditions, and ensure precision materials processing just as efficiently for many materials.

The present paper presents the effects of irradiation of materials using ps laser pulses. The materials investigated were a metal (stainless steel) and a semiconductor (silicon), both of great interest in applications.

2. EXPERIMENTAL SET-UP

The laser used was a Nd-YVO₄ laser (Lumera Rapid), having a pulse duration of circa 9 ps, and an adjustable power of 0.1 W – 2 W. For the present experiments, powers between 0.1 W and 1.5 W were used. The laser emits at three wavelengths in the IR (1.06 μm), visible (532 nm) and UV (355 nm). The laser beam is p-polarized in the case of the IR and visible radiation, and s polarized for the UV radiation. The pulse repetition rate, which can be varied, was 100 kHz or 250 kHz in the experiments reported here.

Two materials were investigated, which are of interest for laser processing applications: polished stainless steel and crystalline silicon; the differences between the materials properties should lead to different irradiation effects. The laser beam was focused onto the surface of the samples using either an $f = 50$ mm lens, or an achromatic 15.8 mm objective; the samples were positioned in the focus or at various distances from the lens focus. Irradiations were performed in air at atmospheric pressure. Both repeated irradiations of the same position and irradiations as the sample surface is scanned with speeds between 2 mm/s and 40 mm/s (leading to lines) were investigated.

3. RESULTS

The SEM images of the samples obtained indicate both similarities and differences between the two materials under investigation. One of the characteristic features we have observed for both materials are ripples (Fig. 1), having a shape

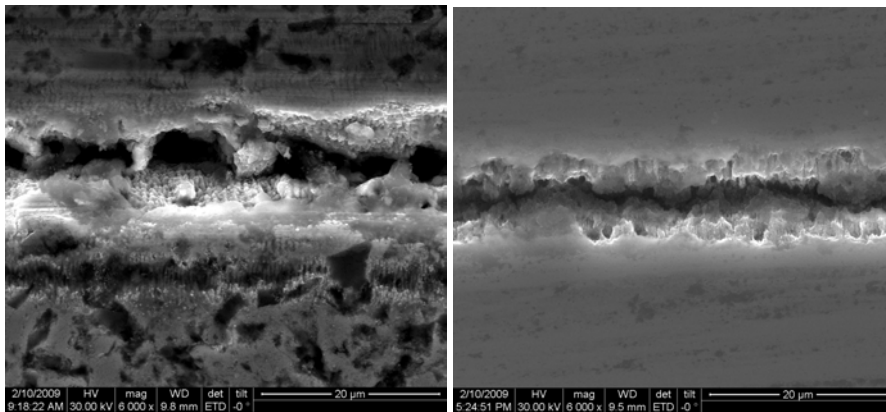


Fig. 1 – SEM images of ps laser-irradiated samples. Left: stainless steel; right: silicon.

similar to that observed by other authors [8]. The ripples are less clear in some cases for the silicon samples, being covered by the surface melt which occurs for this material. Some irregularities in the ripples are the probable result of irregularities at the surface of the irradiated probes, since the formation of the ripples is related to scattering of the laser beam on irregularities of the sample surface, as will be discussed in the following section. The ripples can be observed in the depth of the material, too, not only on the surface. In the case of lines, the ripples observed are always perpendicular to the direction of the line. However, in the case of the lines obtained by scanning at low speeds, or in the case of separate holes, some ripples are observed which deviate laterally inside the line, or converge towards the bottom of the hole. An interesting effect we have observed in some cases is the occurrence of 2 or more rows of clearly separated ripples, having the same periodicity.

In the deep lines resulting from repeated irradiation along a given direction, an asymmetry of the top and bottom of the line is visible (Fig. 2), which is more pronounced for lines obtained using a larger number of passes along the same direction. The thickness of the line is larger on the bottom, as is the amount of material redeposited at the edge of the cut. Although the structure and appearance of the lines in the case of stainless steel and silicon are different, the fact that the asymmetry is the same is significant, and will be discussed later.

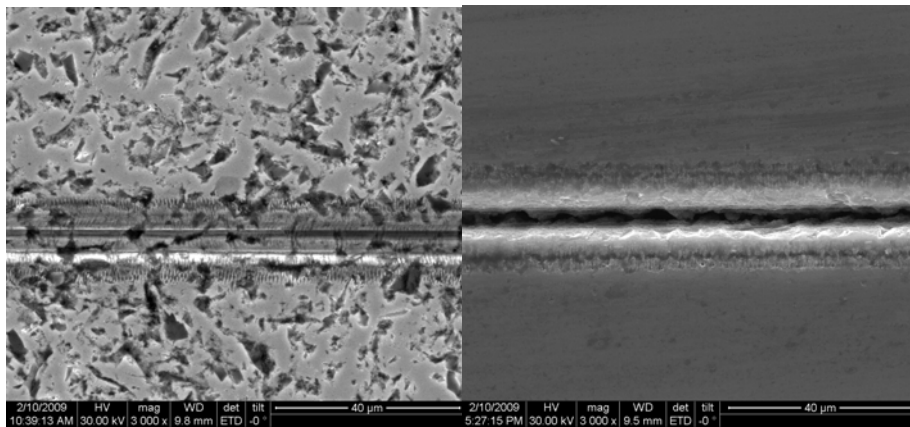


Fig. 2 – Asymmetry of lines obtained for repeated scanning over sample surface.
left: stainless steel; right: silicon.

The visible difference between silicon and stainless steel is the fact that in the case of silicon there is a larger amount of melted and resolidified material in the irradiated lines, which makes the ripples less clear than in the case of steel. This is a result of the different ablation regimes for the two types of materials, which will be treated in the next section. Silicon also presents more chipping and cracks, as a result of the same effect, as is apparent in Fig. 3. The chipping is due to large scanning speeds, which lead to incomplete drilling and the burst effect of the ablation plasma.

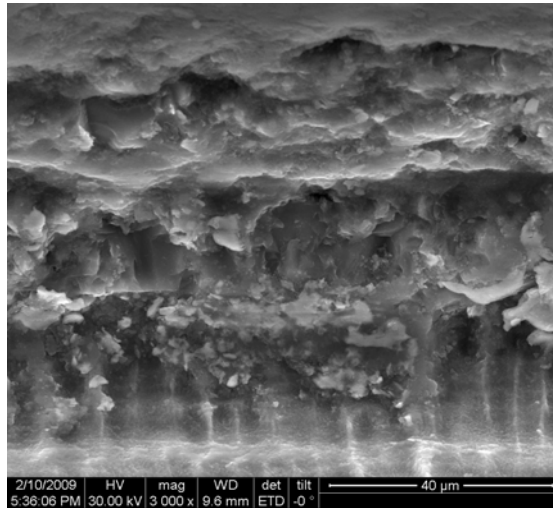


Fig. 3 – Typical structure for silicon with chipping, melting and resolidification of ablated material.

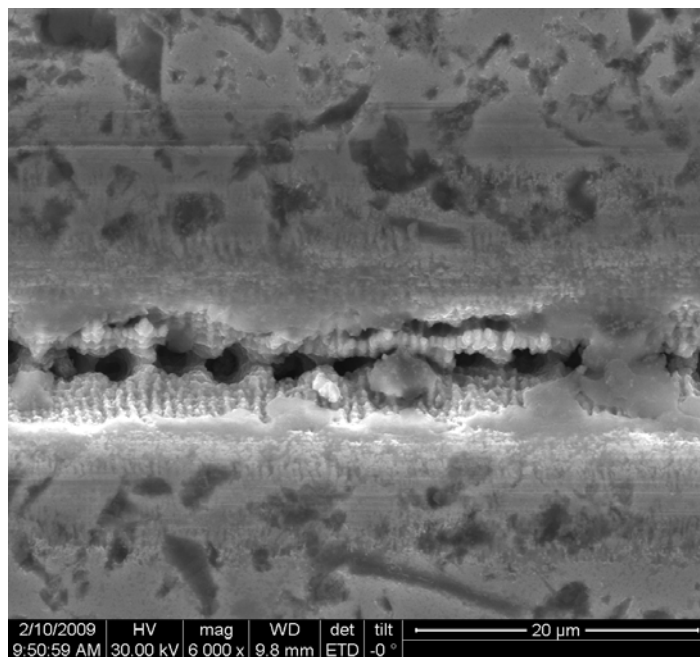


Fig. 4 – Structure for stainless steel with cones in a regular matrix in the depth of the ablated line.

Stainless steel, on the other hand, presents in some conditions cone structures in a regular matrix (Fig. 4); we speculate that these are a result of the bidimensional ripples, since in the cases when a well-separated cone structure is observed (in the absence of holes), ripples are visible in depth, as can be seen in Fig. 5.

The structure of the lines depends on the scanning speed. For lower speeds, separated holes (none penetrating completely to the other side) are visible (see Fig. 4), while for higher speeds, the lines are uniform along their length, with no variations (Fig. 2 left). This is to be expected, since the relationship between the scanning speed and the laser repetition rate, along with the dimension of the spot, determines the degree of pulse overlap and thus the structure of the irradiated region. This will also lead to the existence of an optimum, which will depend on the specific processing application in view.

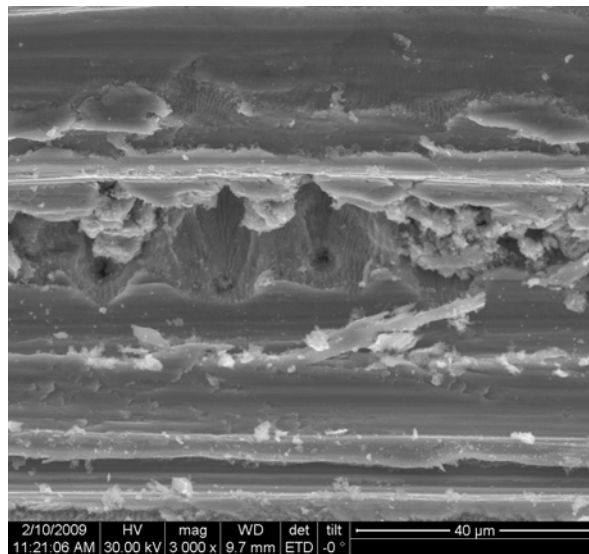


Fig. 5 – Structure of ripples observed in the depth of the holes drilled in stainless steel.

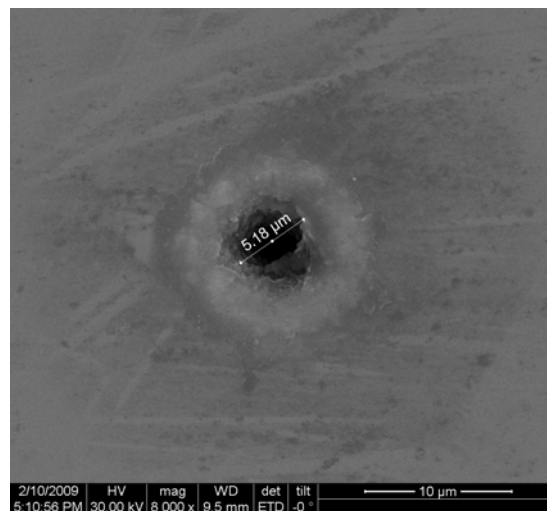


Fig. 6 – Hole drilled in silicon using 10 pulses at 0.5 W power and 100 kHz, with UV radiation.

In the case of holes obtained through multiple pulse irradiation of the same spot, dimensions of the from several μm , up to tens of μm , can be obtained, as exemplified in Fig. 6 for silicon; the symmetry of the holes is relatively good. Both in the case of silicon and in the case of stainless steel, thin, deep holes associated with fracture and, possibly, with a keyhole effect, are present. The depths of these fractures can be quite large compared to the hole diameter (for example, a 60 μm depth hole having a 7 μm diameter). These can be tentatively explained by melting, followed by vaporization of the material and expulsion of the melt by the motion of the vaporized material.

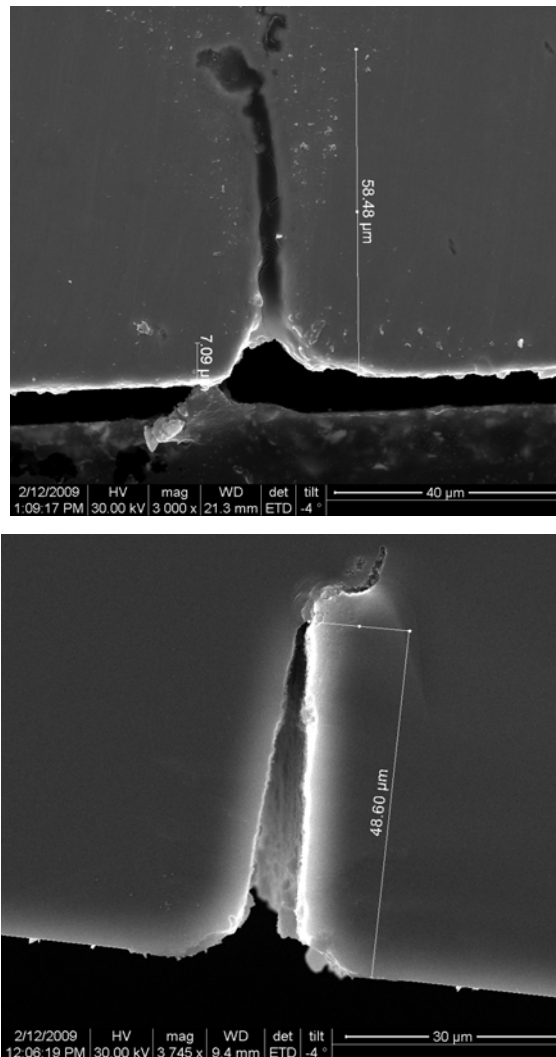


Fig. 7 – Section of holes drilled in stainless steel (top) and silicon (bottom).

4. DISCUSSION

Some of our irradiated samples, both stainless steel and silicon, present ripples, as mentioned in the above section. Ripples are characteristic structures which have been observed in the interaction of laser radiation with matter for various materials, from mid IR to blue wavelengths of the laser radiation, and for pulse durations from fs to cw radiation [9–11]. Ripples are formed by the interference between the incident laser beam and the part of the laser beam which is scattered on surface defects. A constructive interference region corresponding to maximum energy transfer into the material generates equidistant intensity fringes. As a result, a periodic exceeding of the melting (or equilibrium vaporization) threshold occurs, leading to alternating regions of different crystallinity. The appearance of the ripples is influenced by the presence of surface defects such as grain boundaries.

The periodicity of the ripples is of the order of the wavelength of the incident radiation in the case of metals or other materials having a metallic behavior over the duration of the laser pulse (as a result of the formation of conduction electrons by multiphoton absorption). More specifically, the periodicity depends on the angle of incidence, being approximately equal to the wavelength for normal incidence, and depending on the angle of incidence and the beam polarization in general. Ripples do not appear for a single pulse, only for multiple irradiation of the same spot, since they are associated with a positive feedback phenomenon.

In our case, the ripples are equidistant for the same irradiated lines, being different for lines obtained in different irradiation conditions. This can be explained by the different polarization directions of our laser for different wavelengths, in view of the fact that polarization affects the ripples.

A phenomenon which accounts for the fact that the lines obtained by irradiation have different morphologies, depending on the number of scans over the same region, or on the degree of superposition of the laser spots on the surface, is that of incubation [12]. Incubation is the decrease of the ablation threshold with number of incident laser pulses. This decrease can be described by a power law (1):

$$\Phi(N) = \Phi(1) \cdot N^{\xi-1}, \quad (1)$$

where $\Phi(N)$ is the threshold for ablation after N pulses, $\Phi(1)$ the threshold for a single pulse, and ξ is a coefficient which depends on the material.

Although incubation is present for different types of materials, the mechanisms leading to it are not the same. For metals such as stainless steel, it is due to an accumulation of plastic deformation; for semiconductors such as silicon the source is defects induced by laser irradiation. The amount by which the threshold decreases depends on the material, the pulse duration and the wavelength. For example, in the case of silicon irradiated using 100 fs pulses at 800 nm, the threshold decreases 2 times from the first pulse to the 100th [12]; for

steel irradiated with 150 fs pulses at 775 nm, the threshold decreases by a factor of 3.6 from pulse 1 to pulse 10,000 [13]. A result of incubation is the fact that, due to the decrease of the threshold, the diameter of the ablated hole increases with the number of pulses.

Polarization is an important factor which influences the interaction between picosecond pulses and a given material. In our results, for both types of materials studied, as can be seen in Fig. 2, there is an asymmetry in the deep channels resulting from repeated passes along the same line, and this can be ascribed to polarization. The effect of polarization is due to the dependence of the reflection on polarization, as the Fresnel formulas for reflection differentiate for s and p reflected light [14]. The difference in reflection is maximum for angles of incidence of 70–80°. The shape of the hole obtained by irradiation for a stationary beam and target will depend on the polarization. The hole will be circular only in the case of circular polarization [15]. For linear polarization (such as our case) deviation from a circle is larger for smaller energies per pulse, as has been noted by authors using pulses of hundreds of fs duration [16], and decreases with increasing energy density. The fact that the shape of the hole depends on polarization has several implications. First of all, there is a dependence of the shape of the hole or the line on the relationship between the polarization direction and the scanning direction. During the motion, successive spots are superposed differently depending on their shapes (which in turn depend on polarization). As a result, the incubation effect on the superposed portion is different for different shapes. Secondly, the depth of the hole depends on the polarization (due to the superposition and shape). In conclusion, for our case of linear polarization, in order to obtain thin lines, the optimum irradiation conditions is scanning along the direction in which the spot is longer, which will lead to thinner lines and a lower threshold (due to the increased degree of superposition of the spots and the lowering of the threshold). However, for complicated contours, a circular polarization is the optimum one.

Due to the typical distribution of laser intensity in the spot (with the highest intensity in the center), the lateral walls of the holes are not vertical (see Fig. 7), a fact which is undesirable in many applications. This effect cannot be eliminated in our current experimental conditions. The improvement of the hole symmetry can be obtained either by using circular polarization rather than the linear one of the laser beam (by inserting a quarter wave plate in the beam) or by polarization trepanning, which is a rotation of the polarization direction of the existing linear polarization, with speeds of the order of thousands of rpm [17].

In the case ultrashort-pulse irradiation of metals (or materials which have a metallic behavior during laser irradiation as a result of the formation of conduction electrons, such as semiconductors), there are more possible ablation regimes [18]. For energy densities situated a little over the threshold for ablation, the ablation rate is small. This is the “gentle” ablation regime, corresponding to normal vaporization. The irradiated surface is relatively smooth in this case, and ripples are

formed. The “strong” ablation regime appears for larger fluences, but it is also an effect of multiple pulses, since the threshold is lowered due to incubation, and the same energy density becomes much larger than this threshold. The ablation rate increases in this regime, and the irradiated surface is rougher. This is due to the presence of phase explosion at such energy densities. In our case, the regimes for silicon and stainless steel appear to differ; since the threshold for ablation for silicon is lower than that for stainless steel, for the same laser energy density, silicon is, as the figures seem to suggest, in the strong ablation regime, while stainless steel is in the gentle regime. Silicon also presents more chipping; this is due to the appearance of cracks from thermal shock [19]. Chipping is a result of incomplete drilling of the hole, combined with the burst effect of the plasma, which leads to an explosive removal of the material, typical for the strong ablation regime.

Debris is present in all of our irradiated samples, although in varying degrees. The amount of debris accumulated in and around the hole depends greatly on the duration of the laser pulse. The amount of debris is considerably reduced for pulses of hundreds of fs duration, compared to those of ps duration [20], this being one of the areas in which femtosecond lasers are preferable over ps lasers. However, an improvement of the results using ps lasers is possible, if the irradiations are carried out in vacuum. Cutting and drilling of materials in vacuum is known to produce “cleaner” cut edges [21]. Another option, which we intend to study in the future, and which is easier to apply in industrial conditions, is the use of an assist gas.

5. CONCLUSIONS

Stainless steel and silicon samples were irradiated using ps laser pulses in air at atmospheric pressure, various laser powers (energies/laser pulse) and scanning speeds being investigated. SEM images of the samples indicate both similarities and differences between the metal and the semiconductor.

Both of the materials present characteristic ripples, but in the case of silicon these are partly masked by a larger amount of melt. The ripples are present in the depth of the samples, not only on their surface.

A characteristic asymmetry of the top and bottom of the lines appears both in the case of stainless steel and in that of silicon, and is probably due to laser beam polarization effects.

Notable differences for the case of silicon are the larger amounts of melted and resolidified material, and the increased presence of chipping and cracks, due to the “strong” ablation regime for this case (associated with the lower ablation threshold). Steel has, in some cases, a regular pattern of cones which does not appear for the semiconductor. An interesting effect present for both types of materials is the presence of thin holes having several tens of micrometer depth, at diameters of the order of several micrometers.

Holes and lines of several micrometer dimensions (width) can be obtained with such picosecond pulses. An improvement of the beam polarization and ambient gas conditions could lead to cleaner, more abrupt edges of the ablated zone, and thus to a better materials processing quality.

REFERENCES

1. J.F. Ready, *Journal Appl. Phys.*, **36**, 2, 462–468 (1965).
2. S.I. Anisimov, D. Bauerle, B. S. Luk'yanchuk, *Phys. Rev.*, B **48**, 16, 12076–12081 (1993).
3. D.B. Geohegan, A.A. Puretzky, *Appl. Surf. Sci.*, **96-98**, 131–138 (1996).
4. E. Coyne et al, *Appl. Phys.*, A **81**, 371-378 (2005).
5. W. Kautek, P. Rudolph, G. Daminelli, J. Krueger, *Appl. Phys.*, A **81**, 65-70 (2005).
6. A. Weck, T.H.R. Crawford et al, *Appl. Phys.*, A **90**, 537–543 (2008).
7. D. Ashkenazi et al, *Appl. Surf. Sci.*, **120**, 65–80 (1997).
8. S.E. Clark, D.C. Emmony, *Phys. Rev.*, B **40**, 4, 2031–2040 (1989).
9. Z. Guosheng, P. M. Fauchet, A.E. Siegman, *Phys. Rev.*, B **26**, 10, 5366–5381 (1982).
10. A. Weck et al, *Appl. Phys.*, A **89**, 1001–1003 (2007).
11. A.Y. Vorobyev, V.S. Makin, C. Guo, *Journal Appl. Phys.*, **101**, 034903 (2007).
12. J. Bonse, S. Baudach, J. Krueger, W. Kautek, M. Lenzner, *Appl. Phys.*, A**74**, 19–25 (2002).
13. P.T. Mannion et al, *Appl. Surf. Sci.*, **233**, 1-4, p. 275–287 (2004).
14. Y.F. Lu, T.E. Loh, B.S. Teo, T.S. Low, *Appl. Phys.*, A **58**, 423–429 (1994).
15. P.S. Banks et al, *Appl. Phys.* A**69** (Supplement), S377–S380 (1999).
16. K. Vankatakrishnan et al, *Journal Appl. Phys.*, **92**, 3, 1604–1610 (2002).
17. S. Nolte et al, *Appl. Phys.*, A**68**, 563–567 (1999).
18. T.H.R. Crawford, A. Borowiec, H.K. Haugen, *Appl. Phys.*, A**77**, 237–242 (2003).
19. N. Baersch, K. Koerber, A. Ostendorf, K.H. Toenshoff, *Appl. Phys.*, A**77**, 237–242 (2003).
20. C.Y. Chien, M.C. Gupta, *Appl. Phys.*, A**81**, 1257–1263 (2005).
21. T. Matsumura, A. Kazama, T. Yagi, *Appl. Phys.*, A**81**, 1393–1398 (2005).